Theory of extended x-ray absorption edge fine structure (EXAFS) in crystalline solids*†

C. A. Ashley and S. Doniach

Department of Applied Physics and Stanford Synchrotron Radiation Project,† W. W. Hansen Laboratories of Physics, Stanford University, Stanford, California 94305

(Received 8 July 1974)

A general theory of the extended x-ray absorption edge fine structure is given within the framework of a one-electron approximation. An approximate evaluation of this theory is proposed which allows a simple calculation of the spectrum starting from theoretically calculated electron-atom scattering phase shifts. This is shown to agree quite well with the observed spectrum for copper in the energy range 200–800 eV above the K edge without the use of any adjustable parameters. A qualitative evaluation of multiple scattering effects in the general theory is made which should be reasonably good below 100 eV. Multiple scattering corrections are found to be very important in the low-energy region of the spectrum for close-packed structures. It is shown that significant cancellation of single scattering amplitudes can occur which could account for detailed anomalies in the spectrum of Cu found by Stern, Sayers, and Lytle.

I. INTRODUCTION

Recent improvements both in experimental extended x-ray absorption edge fine-structure (EXAFS) data and in their interpretation, due to Sayers, Lytle, and Stern[1] and the promise of greatly increased data rates with a synchrotron source[2] point to the need for a quantitative microscopic theory of this potentially useful analytic tool.

In this paper we establish a multiple scattering theory of EXAFS which is general within a one-electron muffin-tin treatment of a solid.[3] In the higher-energy range of the EXAFS data (a few hundred electron volts above an absorption edge) we propose an approximate form for the evaluation of the general formulas which allows us, with the help of *ab initio* calculations of electron-atom phase shifts, to make a completely parameter-free prediction of the EXAFS spectrum. In the one case where we happen to have access to a reasonably complete set of phase shifts (due to Jepsen *et al.*),[4] namely, copper, we show that the parameter-free formula provides a semiquantitative fit to the observed spectrum in the range 200–800 eV above the K edge. Since the phase shifts for electron-atom scattering in this energy range are mainly determined by the potential in the interior of the atom, we expect a similar approach to work for any material.

The plan of the paper is as follows. In Sec. II we set up the general multiple scattering formalism, following the approach to low-energy-electron-diffraction (LEED) calculations due to Beeby and others. In Sec. III we present our ansatz for the approximate treatment of the high-energy regime. This is applied to the calculation of spectra for both copper and germanium, although the absence of *ab initio* phase shifts for Ge makes the case less reliable. In Sec. IV we go back to the general theory and evaluate multiple scattering effects explicitly in a low-energy regime where only s-wave electron-atom phase shifts need be considered. We show the importance of the geometry of the solid in determining the size of the multiple scattering corrections: For Cu with twelve first-shell neighbors, the first-shell multiple scattering is equal in magnitude to the second-shell single scattering and opposite in sign over the range 0–150 eV. In Ge with only four first-shell neighbors, the multiple scattering corrections are correspondingly weaker.

II. GENERAL THEORY

The physical mechanism of the EXAFS oscillations has been studied for many years[5] (dating back to Kronig[6(a)]). The basic mechanism is interference between the outgoing photoelectron wave from the absorbing atom and the backscattered waves from the surrounding atoms.

In order to write down a theory of this mechanism, we need to say something about the many-electron relaxation processes which take place during the ejection of the inner-shell electron by the x-ray photon.

In this paper we make the basic physical assumption that the interference effects are produced by those events in which the electrons in and around the absorbing atom are *fully relaxed*. This assumption (which we have not proved explicitly) is made plausible by remarking that the interference requires phase coherence between the outgoing and diffracted electron waves. Events in which shake-up occurs will in general lose phase information to the accompanying excitation (plasmons, electron-hole pairs) and so may be expected to provide a broad background absorption, but in general should not contribute to the fine structure. For metals

the final-state potential of the ionized absorbing atom will be fully screened. In insulating crystals, screening will only be partial, owing to dielectric relaxation, so that the low-lying part of the spectrum above the edge will be Coulomb-like. In the following treatment we assume that the scattering of the electron from the ionized atom can be treated in terms of the phase shifts (fully screened case). We also neglect final-state singularity effects which occur right at the absorption edge.

The general x-ray absorption cross section is given by

$$\sigma_a = \tfrac{4}{3}\pi^2 \alpha\, h\nu \sum_f |\langle f|\vec{r}|i\rangle|^2 \delta(E_i - F_f + h\nu) , \quad (1)$$

where α is the fine-structure constant and $h\nu$ is the energy of the absorbed photon. In a single-particle model, the initial state $|i\rangle$ is the core state from which the photoelectron is emitted, and $|f\rangle$ represents the final state of the photoelectron, which must be above the Fermi level. More generally, inelastic scattering will be expected to add an imaginary part to the final photoelectron energy.[6(b)] (The effect of this will be discussed later.)

In order to solve the problem, we need a model to describe the effective potential seen by the final-state photoelectron. We shall assume a simplified model in which this potential can be represented by a nonoverlapping system of spherically symmetric spin-independent muffin-tin potentials, centered about each atomic site. The potential between the muffin tins is assumed to be constant, and this level determines the zero of energy. We further assume that, apart from the central atom from which the photoelectron is emitted, all atoms of the system can be represented by the same muffin-tin potential (unless more than one atomic species is present).

To evaluate the cross section in Eq. (1) we require matrix elements of the operator $\hat{\rho}$, given by

$$\hat{\rho} = \sum_f |f\rangle \,\delta(E_i - E_f + h\nu)\langle f| = -\frac{1}{\pi}\,\mathrm{Im}\,G^{(+)}(E) , \quad (2)$$

where

$$G^{(+)}(E) = 1/(E - H + i\epsilon) \quad (3)$$

and H is the effective single-particle Hamiltonian, representing the central absorbing atom and all the surrounding scattering atoms. E is the energy of the photoelectron, measured relative to the absorption edge, so that the photon energy is $h\nu = E + I$, where I is the ionization potential. The increment $+i\epsilon$ defines the relevant Green's function to be that for the outward propagating wave.

It is convenient at this stage to use the angular momentum representation. We expand in terms of a complete set of one-center basis functions $\phi_L^E(\vec{r})$

at energy E and angular momentum L (l, m) which have the form

$$\phi_L^E(\vec{r}) = i^l R_l^E(r) Y_L(\hat{r}) . \quad (4)$$

The $Y_L(\hat{r})$ represent spherical harmonics, and we shall take the radial functions $R_l^E(r)$ to be solutions of the Schrödinger equation at energy E for the potential of the central absorbing atom in the absence of the other potentials. Outside the muffin-tin sphere of the central atom these functions will look like free-electron solutions, but with a phase shift introduced by the presence of the central atom for each partial wave.

The initial state of Eq. (1) is a core state, which we shall write as

$$|i\rangle = \phi_c(\vec{r}) = i^{l_c} R_{l_c}(r) Y_{L_c}(\hat{r}) , \quad (5)$$

where $R_c(r)$ is the radial solution of the atomic Schrödinger equation for a core electron in an $l = l_c$ state. For absorption edges corresponding to a deep core state we can expect the core wave function to be highly localized near the origin, so that the matrix elements for Eq. (1) are evaluated essentially at the origin $\vec{r} = \vec{0}$ of the central atom.

By using these angular momentum expansions, the cross section may be written in the convenient form

$$\sigma_a = -\frac{1}{\pi}\,\mathrm{Im}\!\left(\sum_{LL'} M_{LL'}^{\text{core}} \langle \phi_L^E(\vec{0})| G^{(+)} | \phi_{L'}^E(\vec{0})\rangle \right) \quad (6)$$

The matrix element $M_{LL'}^{\text{core}}$ is given by

$$M_{LL'}^{\text{core}} = \tfrac{4}{3}\pi^2 \alpha(h\nu)\langle \phi_L^E|\vec{r}|\phi_c\rangle\langle \phi_c|\vec{r}|\phi_{L'}^E\rangle . \quad (7)$$

The problem has now been conveniently divided into two parts; first, the effect of the potential of the central atom on the photoelectron which is emitted from its core, as represented by $M_{LL'}^{\text{core}}$; second, the behavior of the photoelectron outside the central atom as it propagates through a system of spherically symmetric nonoverlapping potentials.

The matrix element $M_{LL'}^{\text{core}}$ is calculated by various authors[7] who wish to investigate the atomic photoelectric cross section. The angular part of the overlap integral leads to the dipole selection rules for the transition

$$\left.\begin{matrix} l \\ l' \end{matrix}\right\} = l_c \pm 1 \; ; \quad \left.\begin{matrix} m_l \\ m_{l'} \end{matrix}\right\} = m_{l_c}, \quad m_{l_c} \pm 1 . \quad (8)$$

This will limit the number of partial waves occurring in the sum of Eq. (6). In particular, for K absorption $l = l' = 1$.

Most theories find that above the K edge, $M_{LL'}^{\text{core}}$ falls off approximately as some power of $h\nu$, this power being given by $\tfrac{7}{2}$ in the simplest theories[8] for the medium-heavy elements. In the case of EXAFS, we are normally interested in the energy range for which $E \ll h\nu$, i.e., most of the energy of the absorbed photon goes into the ionization energy I for

the core electron. Thus $M_{LL'}^{\text{core}}$ is only slowly vary-ing as a function of the photoelectron kinetic energy E, and in practice we shall neglect this variation.

The behavior of an electron moving in the presence of a system of nonoverlapping potentials is a prob-lem similar to that arising in LEED calculations, and has been formulated by Beeby[9] and others.[10,11] Essentially one can think of EXAFS as a kind of "spherical LEED." To proceed one expands the outgoing photoelectron wave from the central atom in terms of partial waves about any other scatter-ing center. The individual electron-atom scatter-ing is then treated exactly in terms of the t matrix appropriate to the muffin-tin potential. The result-ing scattered wave is then re-expanded about the next scattering center. The full Green's function de-fined relative to two scattering centers at $\vec{R}_\alpha$ and $\vec{R}_\beta$,

$$G_{LL'}(\vec{R}_\alpha, \vec{R}_\beta) = \langle \phi_L(\vec{r} - \vec{R}_\alpha) | G^{(+)} | \phi_{L'}(\vec{r}' - \vec{R}_\beta) \rangle \ ,$$

(9)

is then found to satisfy the equation

$$G_{LL'}(\vec{R}_\alpha, \vec{R}_\beta) = G_{LL'}^0(\vec{R}_\alpha, \vec{R}_\beta)$$
$$+ \sum_{R_\gamma \neq R_\alpha} \sum_{L''} G_{LL''}(\vec{R}_\alpha, \vec{R}_\gamma) t_{l''}(E)$$
$$\times G_{L''L'}^0(\vec{R}_\gamma, \vec{R}_\beta) \ .$$

(10)

Here $G_{LL'}^0(\vec{R}_\alpha, \vec{R}_\beta)$ are the matrix elements arising when the free-electron Green's function is ex-panded in terms of spherical Bessel functions about the respective centers $\vec{R}_\alpha$, $\vec{R}_\beta$, and so

$$G^0(\vec{R}_\alpha + \vec{r}_\alpha, \vec{R}_\beta + \vec{r}_\beta)$$
$$= \sum_{LL'} G_{LL'}^0(\vec{R}_\alpha, \vec{R}_\beta) J_L(\vec{r}_\alpha) J_{L'}^*(\vec{r}_\beta) \ .$$

(11)

The elements $G_{LL'}^0(\vec{R}_\alpha, \vec{R}_\beta)$ are given in terms of the Gaunt coefficients[12]

$$C_{LL_1L_2} = \int d\Omega \, Y_L^*(\theta, \varphi) Y_{L_1}(\theta, \varphi) Y_{L_2}(\theta, \varphi)$$

(12)

by

$$G_{LL'}^0(\vec{R}_\alpha, \vec{R}_\beta) = -4\pi k \sum_{L_1} C_{L'L_1L} H_{L_1}(\vec{R}_\alpha - \vec{R}_\beta) \ .$$

(13)

The spherical waves $J_L(\vec{r})$ and $H_L(\vec{r})$ arising in Eqs. (9), (11), and (13) are defined in terms of the usual spherical Bessel function $j_l(kr)$, the spheri-cal Hankel function $h_l^+(kr)$, and the spherical har-monics $Y_L(\hat{r})$ by

$$J_L(\vec{r}) = i^l j_l(kr) Y_L(\hat{r}) \ ,$$
$$H_L(\vec{r}) = i^{l+1} h_l^+(kr) Y_L(\hat{r}) \ ,$$

(14)

where

$$k = (2mE/\hbar^2)^{1/2} \ .$$

(15)

Note that asymptotically we have

$$i^{l+1} h_l^+(kr)\big|_{r\to\infty} \to e^{ikr}/kr \ ,$$

(16)

and so

$$H_L(\vec{r})\big|_{r\to\infty} \to (e^{ikr}/kr) Y_L(\hat{r}) \ .$$

(17)

The diagonal t-matrix elements $t_l(E)$ in Eq. (10) were shown by Beeby[7] to be the usual t matrix, re-lated to the phase shifts $\delta_l(E)$ (after correction of Beeby's result by a factor 2) by

$$t_l = -(2ik)^{-1}(e^{2i\delta_l} - 1) \ .$$

(18)

We shall use the label α to denote the central atom, whose origin will be at position R_α. The relevant Green's function for Eq. (5) is then $G_{LL'}(\vec{R}_\alpha, \vec{R}_\alpha)$. Using Eq. (10) for this Green's function, we obtain two terms. The first term will be just $G_{LL'}^0(\vec{R}_\alpha, \vec{R}_\alpha)$, and will represent the photoelectric effect of the isolated atom, which we shall not consider further here. The second term will contain the interference effects of interest for EXAFS. Thus our general formula for the oscilla-tory part of the photoelectric cross section is

$$\sigma_\alpha^{\text{oscil}} = -\frac{1}{\pi} \text{Im} \left(\sum_{LL'} |M_{LL'}^{\text{core}}| e^{i(\eta_l + \eta_{l'})} \right.$$
$$\left. \times \sum_{\beta \neq \alpha} \sum_{L_1} G_{LL_1}(\vec{R}_\alpha, \vec{R}_\beta) t_{L_1}(k) G_{L_1L'}^0(\vec{R}_\beta, \vec{R}_\alpha) \right) \ .$$

(19)

In this expression we have extracted the phase shift $\eta_l + \eta_{l'}$ introduced, via the central atom ma-trix elements, between the outgoing L wave and the incoming L' wave.

From the general form of Eq. (19) it is evident that it represents a summation over the atoms β of backscattered waves from each site, which is a generalization of earlier theories of EXAFS, where the backscattering was not treated in terms of the full Green's function. In our formulation multiple scattering effects are all included in principle by the full Green's function $G_{LL'}(\vec{R}_\alpha, \vec{R}_\beta)$, which con-tains scattering at all other sites in the waves that propagate from α to β. The multiple scatter-ing equations are essentially the same as those of LEED theory, where they have been successfully handled by numerical techniques.

For K-edge absorption, the dipole selection rules give $l = l' = 1$. Analytical evaluation of Eq. (17), however, would be greatly simplified if we dealt with the Green's functions G_{0L} and G_{L0}^0 instead of G_{1L} and G_{L1}^0. Asymptotically, this is equivalent to assuming that the photoelectron wave is spherically symmetric about the central atom. In a material of cubic symmetry, this modification is not expected to give rise to any qualitative differences. It should be noted that for numerical evaluation using the matrix inversion procedures developed in LEED[4] there would be no reason to make such a modifica-

tion. However, for the purpose of physical insight in the next two sections we shall make the simplification and therefore consider the behavior of the function

$$\chi(k) = -\operatorname{Im}\left(e^{2i\eta_1} \sum_{\beta \neq \alpha} \sum_{L} G_{0L}(\vec{R}_\alpha, \vec{R}_\beta) \times t_l(k) G_{L0}^0(\vec{R}_\beta, \vec{R}_\alpha)\right) . \quad (20)$$

This function will be a measure of the EXAFS spectrum in our simplified model, apart from the factors in $M_{LL'}^{core}$, which, as we have argued, will be approximately independent of k. In the rest of the paper we work with the simplified form given in Eq. (20).

III. HIGH-ENERGY REGION

At sufficiently high photoelectron energy, the crystal is relatively transparent, and the amount of scattering at a given site, as represented by the $t(k)$ in Eq. (20), becomes small. In this regime we make a basic assumption that the main effects of multiple scattering will be to attenuate the amplitude in a given outgoing wave by transferring it to other partial waves in a rather complex and, at high enough energies, incoherent manner. In order to estimate this attenuation for a given shell of atoms, we calculate a spherically averaged transmission function for each shell, given by

$$W_j(k) = 1 - N_j \frac{\sigma_T(k)}{4\pi R_j^2} , \quad (21)$$

where N_j is the number of atoms in shell j, at distance R_j from the central atom, and σ_T is the total scattering cross section, including both elastic and inelastic contributions. The latter contribution is the one represented by assuming a complex atomic potential in LEED calculations.[6(b)]

The probability of reaching a given shell without scattering is then given by the product of the transmission functions for the intermediate shells, and we assume that the full Green's function may be rewritten in the form

$$G_{0L}(\vec{R}_\alpha, \vec{R}_\beta) \cong A_j(k) G_{0L}^0(\vec{R}_\alpha, \vec{R}_\beta) , \quad (22)$$

where j is the shell label corresponding to the atom site β, and $A_j(k)$ is the attenuation factor given by

$$A_j(k) = \prod_{p=1}^{j-1} W_p . \quad (23)$$

We define $A_1(k) = 1$ for the first shell. Just how high the energy need be before this approximation becomes reasonable cannot be predicted at this stage, but we shall see in later sections that 200–300 eV is reasonable for elements with Z in the region for copper. With this rather crude approximation we then have from Eq. (20)

$$\chi(k) = -\operatorname{Im}\left(e^{2i\eta_1} \sum_{\beta \neq \alpha} A_{j_\beta} \sum_{L} G_{0L}^0(\vec{R}_\alpha, \vec{R}_\beta) \times t_l(k) G_{0L}^0(\vec{R}_\beta, \vec{R}_\alpha)\right) , \quad (24)$$

where j_β is the shell containing the β atom.

The free-electron Green's functions are given in general by Eq. (13). The asymptotic form is obtained by using Eq. (16) for the Hankel function, and this will be a good approximation at energies $E \gtrsim 100$ eV. Equation (24) then becomes

$$\chi(k) = -\operatorname{Im}\left(e^{2i\eta_1} \sum_{\beta \neq \alpha} A_{j_\beta} \frac{e^{2ikR_{\alpha\beta}}}{R_{\alpha\beta}^2} \sum_{L_1} C_{LL_10} \times Y_{L_1}(-\hat{R}_{\alpha\beta}) \sum_{L_2} C_{0L_2L} Y_{L_2}(-\hat{R}_{\alpha\beta})\right) . \quad (25)$$

The Gaunt coefficients in Eq. (25) are given by

$$C_{LL_10} = (1/\sqrt{4\pi})\delta_{l,l_1}\delta_{m_l,m_{l_1}} , \quad (26)$$

$$C_{0L_2L} = (-1)^{m_l}(1/\sqrt{4\pi})\delta_{l,l_2}\delta_{m_l,-m_{l_2}} ,$$

where the δ's are Kronecker δ functions. If we substitute in Eq. (25) and use the addition theorem for spherical harmonics[13]

$$P_l(\hat{r}' \cdot \hat{r}) = \frac{4\pi}{2l+1} \sum_{M=-l}^{+l} (-1)^M Y_{l_1-M}(\hat{r}') Y_{l,M}(\hat{r}) , \quad (27)$$

where P_l is a Legendre polynomial, we obtain the compact form

$$\chi(k) = \left(\sum_{\beta \neq \alpha} A_{j_\beta} \frac{e^{i(2\eta_1 + 2kR_{\alpha\beta})}}{R_{\alpha\beta}^2} f(\pi)\right) , \quad (28)$$

where the scattering amplitude $f(\theta)$ is defined in the usual way:

$$f(\theta) = \frac{1}{2ik} \sum_{l=0}^{\infty} (2l+1)(e^{2i\delta_l} - 1) P_l(\cos\theta) . \quad (29)$$

Our expression for the EXAFS spectrum from Eq. (28) now becomes

$$\chi(k) = \left(f(\pi) \sum_{j} \frac{N_j}{R_j^2} e^{i(2\eta_1 + 2kR_j)} A_j(k)\right) , \quad (30)$$

where the summation is now over shells j.

The form of Eq. (28) is similar to that used by Sayers et al.[1] and earlier authors. However there are two physically important generalizations in our form which have a considerable effect on the resulting fit to experiment. One is that we use the full t matrix to determine the backscattering amplitude $f(\pi)$. We show below that the energy dependence of both the amplitude and phase of $f(\pi)$ are important. The second is that we allow an energy-dependent penetration of the electrons to distant shells. This will be important in the high-energy regions of the spectrum where electron mean free paths become relatively long and result in high-frequency Fourier components in the interference.

Furthermore our *Ansatz* for $A_j(k)$ allows us to calculate this penetration directly in terms of calculated electron-atom cross sections.

This calculation requires an estimation of the energy-dependent elastic and inelastic cross sections σ_E and σ_I. The former can be evaluated either from the atomic scattering phase shifts, using the optical theorem, or by integration from a model potential form (e.g., screened Coulomb) in the high-energy limit. Calculation of the inelastic cross section is not so straightforward, but LEED work[14(a),14(b)] has indicated that σ_I is sufficiently small in metals (mean free paths of about 10 Å at 100 eV) that we may take σ_E as giving the dominant contribution to the total cross section.

The attenuation coefficient $A_j(k)$ is only defined as a function of r at the discrete values $r = r_j$, a shell radius. In order to get a feeling for the energy dependence of the corresponding photoelectron mean free path, we have fitted the calculated values of $A_j(k)$ to the exponential form $e^{-\gamma r}$ with an energy-dependent parameter γ. γ thus represents the inverse mean free path, and is shown as a function of energy in Fig. 1 for copper and germanium. In the case of copper we have used the scattering phase shifts of Jepsen *et al.*[4] in the low-energy range ($E \lesssim 200$ eV), a screened Coulomb form in the high-energy range ($E \gtrsim 500$ eV), and a smooth interpolation in between. The resultant curve for copper shows an effective mean free path of about 3 Å at 200 eV, increasing to 8 Å at 1000 eV. In germanium we expect the cross section at high energies to be roughly the same as for copper, since their atomic numbers are approximately the same, but this assumption leads, nevertheless, to very different mean free paths because of the different lattice structures. Figure 1 shows that the effective mean free path in germanium is much larger than the corresponding value in copper, because the latter is a more densely packed lattice. We shall see further aspects of this contrast in

FIG. 2. Energy dependence of backscattering amplitude $f(\pi)$ calculated using phase shifts of Jepsen *et al.* (Ref. 2).

Sec. IV, when we look in detail at the multiple scattering effects.

We have also shown in Fig. 1 the corresponding value of γ in copper using the inelastic cross section σ_I (as given by the work of Jepsen *et al.*[14(a)] This shows that σ_E does indeed dominate the attenuation. The single scattering formula for the EXAFS [Eq. (30)] now becomes

$$\chi(k) = |f(\pi)| \sum_j \frac{N_j}{R_j^2} \sin(2kR_j + \alpha) A_j(k) e^{-\sigma_j^2 k^2/2} . \quad (31)$$

We have included a simple Debye-Waller factor similar to that used by Sayers *et al.*,[1] σ_j^2 being a measure of the mean-square fluctuations of the actual positions of the atoms in the jth shell about their average positions $\vec{r}_j$. The phase angle α is given by

$$\alpha(k) = 2\eta_1 + \arg[f(\pi)] . \quad (32)$$

The phase shift η_1 corresponds to the central atom, with an effective potential that will be different from that of the other atoms owing to the presence of a core hole, but for simplicity we shall assume that for energies greater than 100 eV, we may replace η by δ, the atomic phase shift. In order to determine $f(\pi)$ we use the phase shifts for the one case (Cu) where we can conveniently make use of the calculations using a self-consistent atomic potential by Jepsen, Marcus, and Jona.[4] When this is done, $\alpha(k)$ is found to be approximately linear in the range 100–300 eV, and given (for copper) by

$$\alpha_{Cu} = 1.9 - 0.42k , \quad (33)$$

where k is in Å^{-1}. The amplitude and phase of $f(\pi)$ for Cu is plotted in Fig. 2. Above 300 eV we have made a smooth extrapolation into the value calcu-
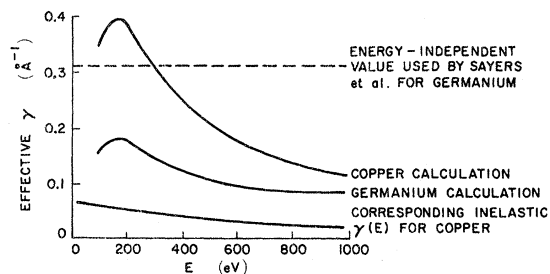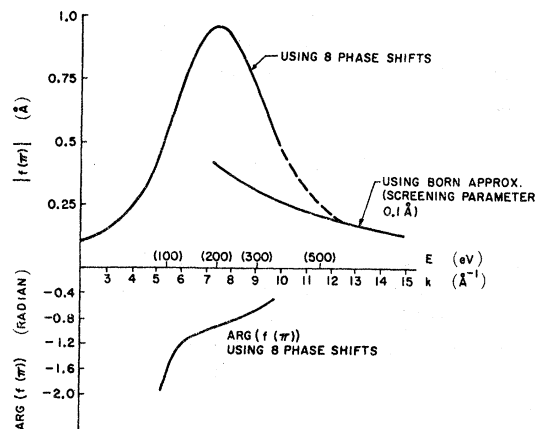

FIG. 1. Penetration of electrons calculated using a spherically averaged transmission function [Eq. (23)] expressed in terms of effective energy-dependent inverse mean free path.

lated from the Born approximation, using a
screened Coulomb potential with screening radius
of order 0.1 Å. For the phase shift α in Eq. (31)
we shall use Eq. (33) over the entire energy range.
The results for Cu are plotted in Fig. 3. The ver-
tical scale in this figure represents the absorption
coefficient (minus the sloping background) in arbi-
trary units, since we have made no attempt to cal-
culate the absolute magnitude of the absorption co-
efficient. The experimental data of Sayers et al.[1]
are shown for comparison on the same scale. We
have shifted the theoretical spectrum slightly to al-
low for the different zeroes of the energy scales —
in our theory we take the muffin-tin zero (also
called "inner potential") in the crystal to be the
zero of energy, whereas the zero for the experimen-
tal curves is the Fermi level. This point is dis-
cussed by Azaroff,[5] who estimates a value of 11
eV for the shift in copper.

The general agreement between experiment and
theory is reasonably good over the range 200–900
eV. It is important to remember that there are no
experimentally fitted parameters in our theoretical
spectrum. This removes one of the limitations of
the earlier theories. The other general improve-
ment is that the envelope of the oscillations is cor-

FIG. 4. Calculation of EXAFS spectrum for Ge using
one empirically fitted phase-shift parameter [Eq. (34)]
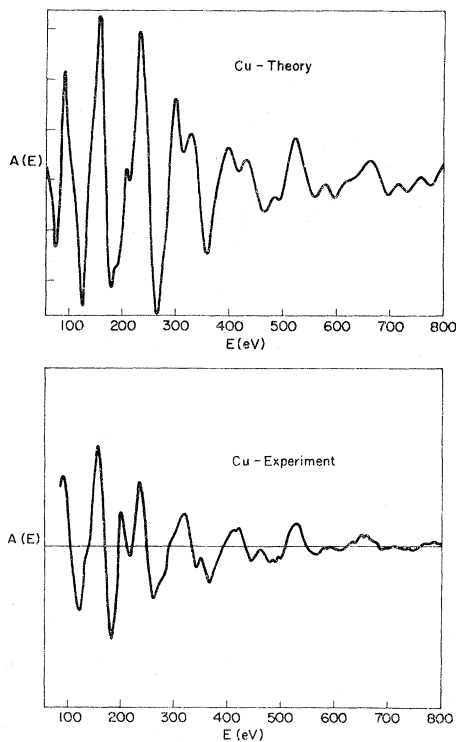compared to data of Sayers et al.

FIG. 3. Ab initio calculation of EXAFS spectrum for
Cu from Eq. (31). (Only the amplitude is arbitrary.)
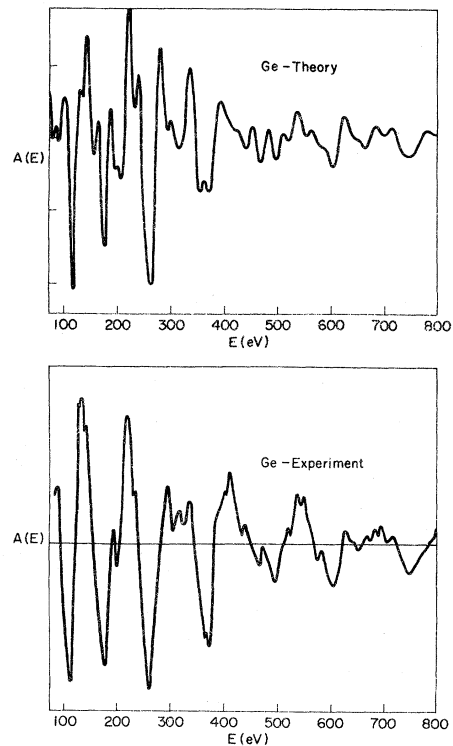The experimental data are from Sayers et al. (Ref. 1).

rectly peaked around 150–200 eV by the form of
$|f(\pi)|$ shown in Fig. 2. Finally, the fact that the
effective mean free path becomes long at higher
energies means that more high-frequency compo-
nents are predicted than in the constant-mean-
free-path calculations of Sayers et al.

For germanium, in the absence of tabulated
phase shifts similar to those for copper, we use
a best linear fit to the primary peaks in the experi-
mental EXAFS spectrum (Fig. 4) and obtain

$$\alpha_{Ge} = 4.5 - 0.41k .\tag{34}$$

We shall assume $|f(\pi)|$ has the same k dependence
as for copper. The resulting theoretical spectrum
(Fig. 4) is reasonably good above 200 eV.

We note that the attenuation in germanium is
predicted to be much less than in copper, mainly
because of the smaller number of nearest neigh-
bors in the former structure. This means that
the contribution to the EXAFS from distant shells
in germanium will be much more important than
for copper. Our theoretical spectrum for ger-
manium shows more fine structure than that of
Sayers et al., especially in the high-energy region
where we predict a mean free path ~ 8 Å rather
than their value of 3–4 Å. (See Fig. 1.) Our ener-

gy-dependent value of γ predicts significant contributions to the EXAFS in germanium from atoms as far out as the fifteenth shell. These features appear to agree with the high-frequency components seen in the observations at high energy (subject to uncertainties about noise).

IV. MULTIPLE SCATTERING EFFECTS

In the previous section we saw how our simple formula, which replaces multiple scattering effects by a penetration probability, works in the higher-energy region of the EXAFS spectrum. The resulting attenuation was shown to be quite sensitive to lattice structure, especially the number of nearest neighbors (first-shell atoms). This attenuation factor was at its largest value at low energies ($E \lesssim 300$ eV), and was sufficient in copper at 200 eV to reduce the amplitude of the outgoing wave from the second shell by 50%. When the first-shell scattering is this strong, it does not seem reasonable to neglect possible structure due to multiple scattering terms, and we must look at these terms in detail. This is certainly the case in LEED calculations, where the inclusion of the full multiple scattering effects has been essential to obtaining agreement with the experiments.

The full Green's function that includes multiple scattering is given by the solution of Eq. (10), and to solve this equation in general will require matrix inversion, which has been successfully performed in LEED using numerical techniques. The dimensions of the matrices involved depend on the number of non-negligible phase shifts in the energy range of interest. LEED calculations in the energy range 0–300 eV tend to use four to seven partial waves. In the present paper we report a trial calculation where only the s-wave ($l = 0$) phase shifts are included. This will be a plausible approximation at low energies ($E \gtrsim 100$ eV), but the main reason for making this assumption is that the problem is then amenable to simple analytical solution for the full

Green's function. We shall find interesting effects that arise as a result of including just the s-wave multiple scattering, and will then discuss the addition of higher partial waves.

For s-wave scattering only, our Eq. (20) for the EXAFS becomes

$$\chi(k) = -\mathrm{Im}\left(e^{2i\eta_1}\sum_{\beta \neq \alpha} G_{\alpha\beta} t(k) G_{\beta\alpha}^0\right) , \qquad (35)$$

where we have dropped the angular momentum labels on G and t since they are always $l = 0$. The equation satisfied by the full Green's function is now, from Eq. (10),

$$G_{\alpha\beta} = G_{\alpha\beta}^0 + \sum_{\gamma \neq \alpha} G_{\alpha\gamma} t(k) G_{\gamma\beta}^0 . \qquad (36)$$

We shall evaluate Eq. (35) for the EXAFS due to the first two shells only. The closest shells tend to dominate the structure in any energy range, but at low energy (above 20 eV for Cu) this seems to be particularly true, owing to the inelastic collision effects being large. In LEED it has been found[14] that the spectrum is insensitive to the addition of further atomic layers beyond the fourth layer. Thus if multiple scattering effects are important in EXAFS, they should appear in the contributions from the closest shells.

For the two-shell problem we shall use a convenient notation where β or β' represents an atom in the first shell, and γ or γ' represents an atom in the second shell. α represents the central atom as usual. In this notation, Eq. (33) becomes

$$\chi(k) = -\mathrm{Im}\left[e^{2i\eta_1} t\left(\sum_{\beta} G_{\alpha\beta} G_{\beta\alpha}^0 + \sum_{\gamma} G_{\alpha\gamma} G_{\gamma\alpha}^0\right)\right] . \qquad (37)$$

The relevant Green's functions $G_{\alpha\beta}$ and $G_{\alpha\gamma}$ are found by application of Eq. (36) and solution of the two resultant coupled equations. This is quite straightforward for s waves and we obtain

$$G_{\alpha\beta} = \frac{G_{\alpha\beta}^0(1 - t\sum_{\gamma' \neq \gamma} G_{\gamma'\gamma}^0) + tG_{\alpha\gamma}^0\sum_{\gamma} G_{\gamma\beta}^0}{(1 - t\sum_{\beta' \neq \beta} G_{\beta'\beta}^0)(1 - t\sum_{\gamma' \neq \gamma} G_{\gamma'\gamma}^0) - t^2(\sum_{\beta} G_{\beta\gamma}^0)(\sum_{\gamma} G_{\gamma\beta}^0)} , \qquad (38)$$

$$G_{\alpha\gamma} = \frac{G_{\alpha\gamma}^0(1 - t\sum_{\beta' \neq \beta} G_{\beta'\beta}^0) + tG_{\alpha\beta}^0(\sum_{\beta} G_{\beta\gamma}^0)}{(1 - t\sum_{\beta' \neq \beta} G_{\beta'\beta}^0)(1 - t\sum_{\gamma' \neq \gamma} G_{\gamma'\gamma}^0) - t^2(\sum_{\beta} G_{\beta\gamma}^0)(\sum_{\gamma} G_{\gamma\beta}^0)} . \qquad (39)$$

Note that Eqs. (38) and (39) are symmetric with respect to the interchange β, $\beta' \leftrightarrow \gamma$, γ', and reduce to $G = G^0$ as $t \to 0$, as required. The multiple scattering terms that arise for finite t appear in Eqs. (38) and (39) as products of the form tG^0, which is proportional to the parameter $1/ka_0$, where a_0 is the lattice parameter. This can be seen from the

form of G^0 in Eq. (13), using the asymptotic approximation of Eq. (16), so that we have

$$G_{\alpha\beta}^0\big|_{|\vec{R}_{\alpha\beta}| \to \infty} \to -e^{ik|\vec{R}_\beta - \vec{R}_\alpha|}/|\vec{R}_\beta - \vec{R}_\alpha| . \qquad (40)$$

Although the parameter $1/ka_0$ is small at all energies of interest here, it is not obvious that one can expand in powers of t since the multiple scat-

tering terms also involve summations over the number of atoms in each shell, and there may be large factors involved. We find, however, that the s-wave scattering is not large enough to produce poles in the Green's functions in Eqs. (38) and (39).

Substitution of Eqs. (38) and (39) into Eq. (37) gives the s-wave contribution to the EXAFS spectrum for two shells. The input data for a given material are the phase shifts δ_0 and η_1 and the structure and lattice parameters. The results for copper and germanium are shown in Figs. 5 and 6. In order to assess the relative importance of each contribution, we have plotted separately the contributions to $\chi(k)$ from the first-shell single scattering, second-shell single scattering, and multiple scattering only terms in Eq. (37). For each material these contributions are plotted on the same scale, and the sum of the three will give the total two-shell s-wave EXAFS at low energy. The phase shifts δ_0 and η_1 used in plotting Figs. 5 and 6 were the same as those used for copper in the previous section. We again took the phase shifts for germanium to be the same as for copper, and while this is an unlikely assumption at low energy, the relative magnitudes of the multiple and single scattering terms are not very sensitive to the phase
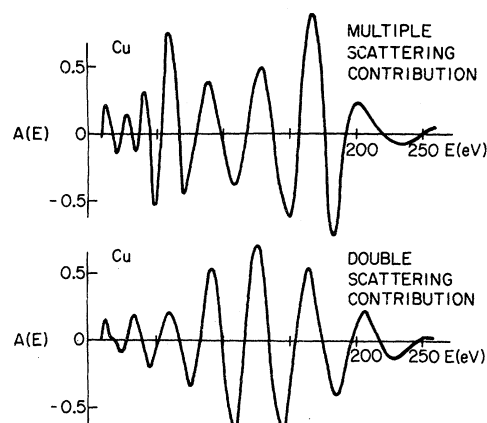
FIG. 6. This shows how multiple scattering effects are much weaker in Ge than in Cu owing to the much smaller number of first-shell neighbors in the Ge lattice (four as opposed to twelve for Cu).

shift chosen. The main effects of changing the phase shifts would be to move the positions of the peaks along the energy axis and to shift the position of the maximum of the envelope by the same amount for each contribution to the spectrum. For the present purpose of gathering physical insight, the lack of accurate phase shifts for germanium is acceptable.

Comparing the multiple scattering contributions for copper and germanium, we see that the magnitude of this contribution in copper is approximately twice that for germanium. This effect is purely a manifestation of the structural difference between the two lattices, specifically the fact that copper has twelve first-shell atoms and germanium has four. The scattering by the first shell of copper is very strong and leads to strong multiple scattering effects.

Moreover, the second-shell single scattering contribution in copper is relatively small because there are only six atoms in this shell (in germanium there are twelve). The strong multiple scattering contribution is actually larger than the second-shell single scattering contribution in copper, as can be seen from Fig. 5, where they are plotted together. It is also significant that the multiple scattering contribution is almost exactly 180° out of phase with the second-shell contribution over most of its energy span. This effect is a possible explanation for the anomalous results found by Sayers et al.[15] for copper. They found an apparent sign reversal between the EXAFS contributions due to the first and second shells, using a simple single scattering formula similar to Eq. (30). Our analysis shows that strong multiple scattering in copper can lead to an appreciably large contribution to the
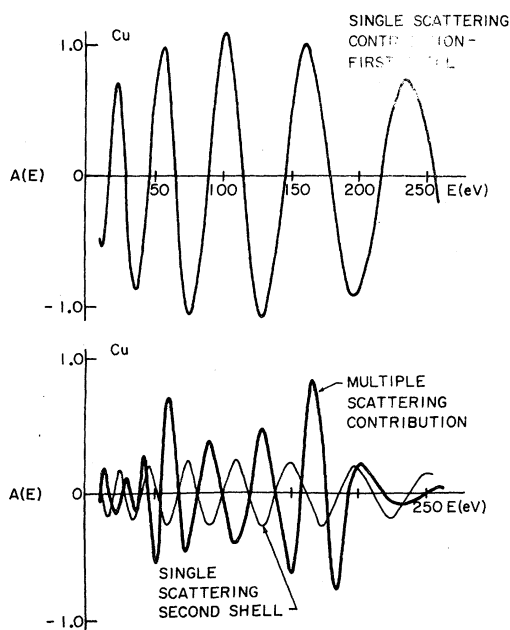

FIG. 5. Comparison of single and multiple scattering contributions for Cu obtained from an s wave only, two-shell evaluation of the general theory. The large cancellation between second-shell single scattering and first-shell multiple scattering might account for the anomalies observed by Sayers et al. (Ref. 15) for Cu.

EXAFS with the same periodicity as the second-shell contribution, but almost exactly out of phase with it. Cancellation would occur between the two and the result might very well look like a second-shell single scattering term with sign reversal. A more complete calculation involving several phase shifts would be needed to establish this conclusion quantitatively.

Further physical insight into this cancellation effect can be had by examining the double scattering terms, which can be extracted by taking the first-order iterative solution of the Green's function in Eqs. (36) or, equivalently, by expanding Eqs. (38) and (39) to first order in t. Figure 7 shows a comparison of the double scattering and multiple scattering contributions in copper, and it is evident that the former contains the main part of the full multiple scattering expansion. The advantage of considering double scattering terms is that they can be identified with specific scattering paths in the lattice, and we find two main contributions for copper, one of which is the path involving the shortest intrashell scattering in the first shell. This is the contribution that has the same periodicity as the second-shell single scattering term, and so we can see that the possible cause of the copper anomaly is the contrast between the strong multiple scattering within the first shell (twelve atoms) and relatively weak single scattering contribution from the second shell (six atoms). In the case of germanium, the situation is reversed, with only four first-shell atoms and twelve second-shell atoms, so that the single scattering contributions are not so likely to be obscured by multiple
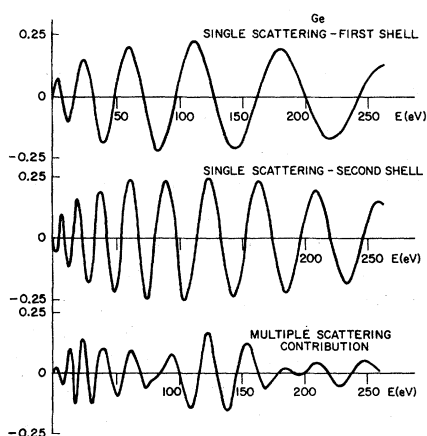
scattering effects. This is consistent with the fact that no sign-reversal anomaly was found by Sayers *et al.* in the case of germanium.

We can make some qualitative observations about the effects of higher partial waves by considering the angular dependence of the scattering amplitude $f(\theta)$ [see Eq. (29)]. The general behavior of the Legendre polynomials means that this function is strongly peaked about the forward scattering direction ($\theta \approx 0°$), with a smaller peak about the backscattering extreme ($\theta \approx 180°$). Since the two-shell multiple scattering paths generally do not involve forward-scattering angles, the use of s waves only (which means spherically symmetric scattering) may be an overestimate of the relative importance of multiple scattering. An alternative approach used by Lee[16] is to consider only the multiple scattering from specific forward-scattering paths, the shortest of which involve first- and fourth-shell atoms in copper. His calculations seem to indicate that strong multiple scattering effects are indeed associated with these selected paths. A full numerical calculation for copper using several ($\gtrsim$ four) partial waves and at least four shells should be possible using the formalism we have developed.

V. CONCLUSIONS

We have developed a general formalism for EXAFS within a one-electron theory, presented in Sec. II, and have seen how the EXAFS spectra for different materials can be calculated in a simple way from first-principles electron-atom phase shifts in terms of a simple formula given in Sec. III. The approximation made there, which involves the calculation of an effective energy-dependent attenuation length for the photoelectrons was seen to work rather well for the one case, crystalline copper, where adequate phase shift data were conveniently available. In Sec. IV we have discussed multiple scattering corrections in terms of a highly simplified solution of the general equations. Our considerations indicate that the attenuated single scattering approximation of Eq. (31) is most likely to be successful for relatively loosely packed structures such as germanium, and most likely to break down for closely packed structures such as copper (and most other metals) in energy ranges where the scattering due to a single atom is large. This is an important point as regards the possible use of EXAFS as a structural probe, as suggested by Sayers *et al.*[17] They showed that, by taking a Fourier transform of a simple formula such as Eq. (31), it is possible to obtain from the data a radial structure function which has peaks corresponding to shell radii from a given central atom. Our calculations suggest that this approach

FIG. 7. Comparison of full multiple scattering compared with simpler to calculate double scattering. It would be much easier to include higher-than-s-wave phase shifts in a double scattering calculation than to perform the full inversion of the multiple scattering Eqs. (10).

would need to be modified to correct for multiple scattering at lower energies in close-packed structures. It is fortunate that many of the interesting amorphous materials and complex molecules where the power of the EXAFS method in determining local structure on an element-specific basis is most promising[18] are indeed loosely packed structures, so that the single scattering approximation of Eq. (31) is most likely to apply.

*Research partly supported by NSF through the Center for Materials Research at Stanford University and by Army Research Office, Durham, North Carolina.

†Based on a Ph.D. thesis, C. A. Ashley (Stanford University, 1974) (unpublished).

‡Supported by NSF under Grant No. GP 39525 in collaboration with U.S. AEC.

[1]D. E. Sayers, F. W. Lytle, and E. A. Stern, *Advances in X-Ray Analysis* (Plenum, New York, 1970), Vol. 13, p. 248.

[2]Experiments under way at Stanford Synchroton Radiation Project (SSRP) by B. Kincaid, P. Eisenberger, and D. Sayers show data rates two to three orders of magnitude faster than those possible with the best available x-ray tube source.

[3]This theory is basically the same as that proposed by W. Schaich [Phys. Rev. B 8, 4028 (1973)]. However the evaluation we propose here is more general than that discussed by Schaich.

[4]D. W. Jepsen, P. M. Marcus, and F. Jona, Phys. Rev. B 5, 3933 (1972).

[5]See review by L. V. Azaroff, Rev. Mod. Phys. 35, 1012 (1963).

[6](a) R. de L. Kronig, Z. Phys. 70, 317 (1931); 75, 191 (1932); 75, 468 (1932); (b) D. W. Jepsen, P. M. Marcus, and F. Jona, Phys. Rev. Lett. 26, 1365 (1971).

[7]R. H. Pratt and H. K. Tseng, Rev. Mod. Phys. 45, 273

(1973).

[8]W. T. Gardy, *Introduction to Electrodynamics and Radiation* (Academic, New York, 1970), p. 207.

[9]J. L. Beeby, Proc. R. Soc. A 279, 82 (1964), and earlier references contained therein.

[10]P. Lloyd and P. V. Smith, Adv. Phys. 21, 69 (1972).

[11]B. L. Gyorffy and M. J. Stott, Solid State Commun. 9, 613 (1971).

[12]See, for example, M. E. Rose, *Elementary Theory of Angular Momentum* (Wiley, New York, 1957), Chap. 3.

[13]See, for example, J. L. Powell and B. Craseman, *Quantum Mechanics* (Addison-Wesley, Reading, Mass., 1961), Chap. 7, Sec. 2.

[14](a) D. W. Jepsen, P. M. Marcus, and F. Jona, Surf. Sci. 31, 180 (1972). (b) For aluminum [Ref. 6(b)] the inelastic contribution to the mean free path is considerably shorter (of order 3 Å) in the low-energy region; so it presumably would not be neglected.

[15]E. A. Stern and D. E. Sayers, Phys. Rev. Lett. 30, 174 1973.

[16]P. A. Lee, in Symposium on Many-Body Theory of High Energy Excitations in Solids, Stanford University, 1974 (unpublished).

[17]D. E. Sayers, E. A. Stern, and F. W. Lytle, Phys. Rev. Lett. 27, 1204 (1971).

[18]S. Doniach, *Proceedings of the Nobel Symposium* (Academic, New York, 1974), No. 24, p. 223.